J Therm Anal Calorim (2017) 128:1251–1263
DOI 10.1007/s10973-017-6107-9

Comparison between the effects of superfine steel slag and superfine phosphorus slag on the long-term performances and durability of concrete

Jin Hu[1]

Received: 12 November 2016 / Accepted: 15 January 2017 / Published online: 27 January 2017

Abstract Superfine particles have been used as mineral admixtures to enhance physical properties, mechanical properties, and durability of concrete in a lot of research. In this study, superfine steel slag (FSS) and superfine phosphorus slag (FPS) were ground to 643 and 657 m^2 kg^{-1}, respectively. The water-to-binder (W/B) ratios were set as 0.45 as well as 0.35, and the cement replacements adopted were 15 and 30%. The effects of FSS and FPS on long-term performance and durability of concrete were investigated. The results show that the increase amplitude of reaction degree of FPS is higher than that of FSS at late age (after 90 days). FPS can improve the pore structure of concrete which is beneficial to the resistance to carbonation and chloride ion penetration for concrete at late age while FSS cannot. FPS is also more advantageous to the development of compressive strength and splitting tensile strength of concrete when compared to FSS at late age. FPS is much more beneficial to the resistance to sulfate attack of concrete while FSS is more disadvantageous to the resistance to sulfate attack of concrete as the replacement ratio increases.

Keywords Superfine steel slag · Superfine phosphorus slag · Long-term performance · Durability

✉ Jin Hu
478428210@qq.com

[1] Sichuan College of Architectural Technology, Deyang 618000, China

Introduction

Mineral mixtures are widely used in concrete to improve the performance of concrete. They can improve the rheological property and stability of fresh concrete [1], increase resistance to sulfate attack, reduce the permeability, and refine the pores structure of the cementitious materials [1–4]. Additionally, mineral mixtures improve workability of concrete and promote the durability of concrete due to the improvement of particle packing, denser interfacial transition zone, optimized pore structure, and low permeability [2–7]. What's more, the use of mineral mixtures is environmental-friendly and economical on account of reduced CO_2 emission and cement content. The most common mineral mixtures are ground granulated blast furnace slag (GGBS) and fly ash [8, 9]. GGBS is a by-product from blast furnaces used to make iron which can make contributions to compressive strength, workability, and durability of concrete [10]. Fly ash is a by-product of burning anthracite or bituminous coal. It is a pozzolanic material containing aluminosilicate glass which is beneficial to concrete, such as improved plasticity, decreased adiabatic temperature rise, reduced permeability, and reduced possibility of alkali silica reaction and sulfate attack [11]. However, with widespread use of such commonly used mineral mixtures like slag and fly ash, it is in urgent need to develop new kinds of mineral mixtures due the shortage of such mineral mixtures mentioned above. As a result, steel slag and phosphorous slag come into use and some research has been put on them.

Steel slag is a by-product of the steel refinery process, and the annual production of it in China is about 30 Mt, with only about 22% utilization rate [12, 13]. The chemical composition of steel slag varies on account of its highly variable production method and raw materials [14]. On the

whole, its chemical composition consists of CaO, SiO_2, Al_2O_3, Fe_2O_3, FeO, and MgO. C_2S, RO phase (solid solution of CaO, FeO, MgO, and MnO), C_3S, C_4AF, C_2F, free CaO, olivine, and merwinite are the common minerals in it [15]. Steel slag has latent hydraulicity due to its silicate calcium minerals. However, the hydration activity of steel slag is very low compared to that of Portland cement due to its slow cooling history and high content of non-active components [16–18]. What should be paid attention to is that steel slag contains about 10% of MgO and 40% of CaO in which there is more than 5% of free CaO. It does damage to soundness of concrete due to the formation of $Ca(OH)_2$ and $Mg(OH)_2$ which will cause volume expansion of 98 and 148%, respectively [12]. Li et al. [19] found that steel slag used as partial replacement of Portland cement in concrete could reduce expansion due to alkali-aggregate reaction. Wang et al. [20] found it was negative for the late property and durability of concrete when GGBS combined with high content of steel slag as mineral admixtures in cement-based materials. Tsakiridis [21] replaced cement with 10.5% steel slag and found that the addition of the steel slag did not have negative effects on the quality of the produced cement including grindability, setting time, compressive strength, and soundness. Guo et al. [22] added steel slag powder to concrete and found that the initial and final setting times were slightly retarded. The dry shrinkage was lower, and the abrasion resistance was better. Additionally, steel slag can also be activated by carbon dioxide (CO_2) to form a strength-contributing, carbonate-bond matrix due to its latent hydraulic [23].

Phosphorous slag (PHS) is an industrial by-product of yellow phosphor production through electric furnace method, and its annual production in China is more than 8 Mt [24, 25]. PHS is mainly composed of SiO_2, CaO, and Al_2O_3, and its total content of SiO_2 and CaO is more than 85%. Therefore, it could be used as a replacement of cement-based material [26]. However, PHS has negative effects on early properties of concrete when used at high replacement levels in that P_2O_5 in PHS has a strong retarding effect on setting time of Portland cement and the content of Al_2O_3 in PHS is insufficient [27]. As a result, chemically activated methods like alkali activators have been used to improve its relatively weaker cementing properties. Allahverdi et al. [28] studied the performance of chemically activated high phosphorous slag content cement and found that the durability was weaker while the compressive strength is higher. Li et al. [29] combined GGBS and PHS as a composite mineral admixture in cement-based materials and found that the composite binder with 70% blended materials could reach 52.5-grade slag cement standard and the setting time was shortened greatly. The resistance to sulfate attack of it was found superior to that of Portland cement. Meanwhile, it was confirmed that chemically activated high phosphorous slag content cement presented a significantly better resistance against frost-salt attack [28].

Mechanical grinding is an effective method to improve the activity of mineral admixtures. There are numbers of researchers working on superfine particles used as mineral admixtures to enhance physical properties, mechanical properties, and durability. Her and Lim [30] studied the influence of rapidly chilled and air-cooled nano-slag as a mineral admixture on the properties of mortar. They found that the improvement of fitness of slag could reduce fluidity and increase strength. It was proved by Lim [31] that addition of nano-slag modified the microstructure and improved the strength of concrete. At present, with the progress of grinding technology and the use of high-efficiency grinding agent, it has become easier to obtain ultrafine mineral admixtures. As for steel slag, the specific surface is generally in the range between 300 and 500 $m^2\ kg^{-1}$ when it is used as a mineral admixture, which has been proved to be beneficial to its activity [32, 33]. Wang et al. [34] investigated a superfine steel slag with the specific surface area of 786 $m^2\ kg^{-1}$ which was prepared by mechanical grinding. They found that the superfine steel slag exhibits a much higher activity at early and middle ages but a lower activity at late age than the ordinary steel slag. Hu et al. [35] found that fine steel slag powder retarded the hydration of Portland cement at early age due to relative high contents of MgO, MnO_2, P_2O_5 in it. Liu and Li [36] found that increasing fitness of steel slag could not improve the early cementitious properties of cement blended with steel slag, while it could enhance the late cementitious properties significantly. Shi et al. [37] studied ultrafine grinded steel slag with different particle sizes. They found that water requirement and setting time increased with the decrease in the particle size of steel slag. Feng et al. [38] studied the properties of concrete with 20 and 30% superfine steel slag. Similar compressive strength, elastic modulus, and permeability of concrete mixed with 20% superfine steel slag (FSS) to that of pure cement concrete at the ages of both 28 and 90 days were found, while 30% blended FSS concrete showed lower compressive strength, lower elastic modulus, and higher permeability than pure cement concrete. Besides, there are few studies about superfine phosphorus slag (FPS). Cheng [39] had used FPS to take part place of cement and found decreased hydrate heat and early strength of concrete and improvement of durability. Gao [40] replaced Portland cement with appropriate FPS and found that it could decrease the amount of portlandite, increase the amount of C–S–H gel, reduce the harmful pores (larger than 100 nm), make the structure denser, and improve the microstructure and durability of concrete.

The performances of concrete containing FSS or FPS at early age and mid-age (28 days) have been investigated by some researchers. However, the research on long-term performances and durability are very limited. This paper deals with the influence of FSS and FPS on the long-term performances and durability of concrete.

Experimental

Raw materials

The specific surface area of steel slag used in this experiment was 643 $m^2\ kg^{-1}$ while that of phosphorous slag was 657 $m^2\ kg^{-1}$. The chemical composition of steel slag and phosphorous slag is summarized in Table 1.

The XRD pattern of steel slag and phosphorous slag is shown in Figs. 1 and 2. The main active components of steel slag were crystalline substances, including C_3S, C_2S, C_2F. Steel slag also contained RO phase and Fe_3O_4. Phosphorous slag was mainly composed of amorphous substances, while the crystalline substances mostly in it were SiO_2 and C_2S.

Crushed limestone was used as the coarse aggregate for concrete, with particle sizes between 5 and 25 mm. The fine aggregate used for concrete was natural river sand with particle sizes smaller than 5 mm. Superplasticizer of polycarboxylic acid was used as the water-reducing agent to improve the workability of concrete.

Mix proportions

Two different water-to-binder ratios (W/B) of pastes in this experiment were set as 0.45 and 0.35, respectively. For each W/B, the pure cement concrete was used as the reference sample, and mineral admixture replacements adopted were 15 and 30%. The serial number and the mix proportion of each sample are shown in Table 2. The slump of each concrete sample was between 18 and 20 cm by adjusting the dosage of water-reducing agent.

Test methods

Concrete samples of 100 mm × 100 mm × 100 mm were prepared and cured at standard curing room temperature (20 ± 1 °C, relative humidity is higher than 95%) for the compressive strength test, splitting tensile strength test, and chloride permeability test at the age of 90, 360, and 720 days, respectively. The chloride permeability of concrete was tested by measuring charge passed within 6 h according to the method of ASTM C1202 [41].

Two methods were adopted in this paper to conduct the carbonation experiment after the standard curing for 28 days:

1. Natural carbonation: Natural carbonation was performed in natural curing room with the temperature of 20 ± 3 °C and relative humidity of 55 ± 10% for 360

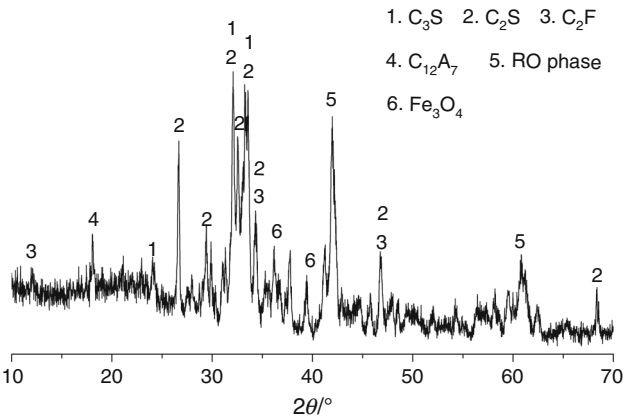

Fig. 1 XRD patterns of steel slag

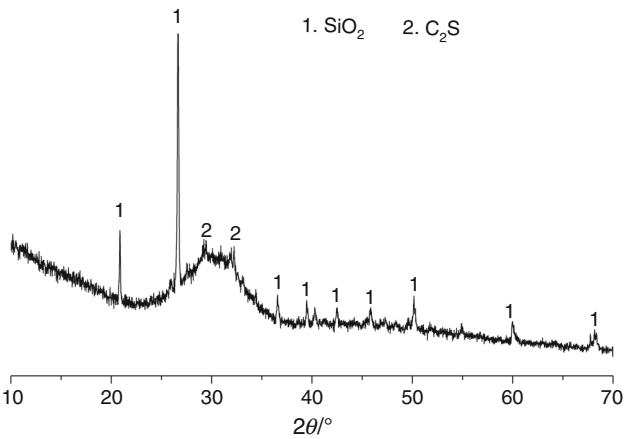

Fig. 2 XRD patterns of phosphorous slag

Table 1 Chemical composition of steel slag and phosphorous slag (*w*/%)

	CaO	SiO_2	Al_2O_3	P_2O_5	MgO	Fe_2O_3	MnO	LOI
Steel slag	39.61	18.56	3.56	1.13	6.98	23.65	2.85	2.11
Phosphorous slag	41.67	39.62	5.12	4.98	1.73	0.37	–	3.69

w—mass fraction LOI—loss on ignition

Table 2 Mix proportions of concretes at W/B ratios of 0.45 and 0.35

Samples	W/B ratio	Mix proportions/kg m^{-3}					
		Cement	Steel slag	Phosphorous slag	Coarse aggregate	Fine aggregate	Water
C-0.45	0.45	340	0	0	1093	824	153
S-0.45-15		289	51	0	1093	824	153
S-0.45-30		238	102	0	1093	824	153
P-0.45-15		289	0	51	1093	824	153
P-0.45-30		238	0	102	1093	824	153
C-0.35	0.35	420	0	0	1099	764	147
S-0.35-15		357	63	0	1099	764	147
S-0.35-30		294	126	0	1099	764	147
P-0.35-15		357	0	63	1099	764	147
P-0.35-30		294	0	126	1099	764	147

and 720 days. The depth of carbonation was measured with the 1% solution of phenolphthalein in alcohol according to the method of GB/T 50082-2009 [42].

2. Accelerated carbonization: The concrete samples were sealed for 90 days in the carbonization box in which the temperature was (20 ± 2)°C, relatively humidity was (70 ± 5) %, and CO_2 concentration was (20 ± 3) % according to the method of GB/T 50082-2009 [42].

The resistance to sulfate attack of concrete was measured by the dry–wet cycling method according to the method of GB/T 50082-2009 [42], and each circulation was within 24 h. The result was characterized by the loss rate of compressive strength K.

$$K = 1 - f_a f_b^{-1}$$

K, The loss rate of compressive strength, %. f_a, The compressive strength of concrete after n times of the dry–wet circulation, MPa. f_b, The compressive strength of concrete at the same age through the standard cure, MPa.

Cement pastes were prepared using moulds of 40 mm × 40 mm × 40 mm, and the moulds were removed after the standard cure for 2 days. After that, the samples were immersed into the saturated $Ca(OH)_2$ solution to prevent carbonation and the precipitation of $Ca(OH)_2$ in hardened cement paste. At the testing age of 90, 360, and 720 days, the samples were immersed in acetone to prevent further hydration. The mineral phases of hydration products were measured by X-ray diffraction (XRD). The mass contents of different hydration products were determined by thermogravimetric analysis (TG). The TG test was performed by using a TA-Q5000 instrument. The heating rate is 10 °C min^{-1}. The sample was heated in nitrogen atmosphere. The pore size distributions were measured by mercury intrusion porosimetry (MIP). Hydration kinetics of cementitious materials in this experiment were characterized by the exothermic rate and the cumulative heat evolved during hydration using a JAF isothermal conduction calorimeter with the temperature of 20 °C.

Results and discussion

Hydration heat

Figure 3 shows the exothermic rate and hydration heat of cement, the composite binder containing 30% superfine steel slag (FSS), and the composite binder containing 30% superfine phosphorus slag (FPS). As shown in Fig. 3a, the hydration evolutions of them are quite similar, which can be divided into five stages: the rapid exothermic period, the dormant period, the acceleration period, the deceleration period, and the steady period. 30% FSS replacement and 30% FPS replacement can both prolong the dormant period, and it is consistent with the findings of Wang et al. [43], Allahverdi and Mahinroosta [44]. The dormant period of the paste containing FPS is comparatively longer than that of the paste containing FSS, which indicates that the presence of P_2O_5 in phosphorus slag results in forming phosphoric acid which reduces the pH of the cementing mixture and provides a negative impact on the rate of the hydration reaction at early age [45]. During the acceleration period, the exothermic rate of the paste containing 30% FPS is reduced remarkably when compared to that of the paste containing 30% FSS, and its second exothermic peak forms later. During the deceleration period, the exothermic rates of the pastes containing 30% FPS or FSS are both higher than that of cement. Two factors may contribute to it. One reason is that cement reacts faster in the acceleration period and its hydration product C–S–H gel is denser which impedes further hydration. Cementing materials mixed with mineral admixtures produce less C–

S–H gel which will have less influence on further hydration. The other reason is that mechanical grinding which increases the fineness of steel slag and phosphorus slag can improve their activity significantly. Therefore, the activity of FSS and FPS is distinctly higher than that of normal steel slag and phosphorus slag at early age, and hence the early reactions of both FSS and FPS make contributions to hydration heat. It is noteworthy that the exothermic rate of the paste containing 30% FPS is superior to that of the paste containing 30% FSS in a long time during the deceleration period. This is mainly because that the retarding effect of FPS on the hydration evolution is more significant than that of FSS before the deceleration period, and thinner C–S–H gel is formed during the reaction of FPS.

As shown in Fig. 3b, the cumulative hydration heat in 3 days of the pastes containing 30% FPS or FSS is lower than that of cement significantly. Meanwhile, the cumulative hydration heat in 3 days of the composite binder containing 30% FPS is slightly lower than that of the composite binder containing 30% FSS. The cumulative hydration heat in 3 days of cement, the paste containing 30% FSS, and the paste containing 30% FPS is 261.8, 232.8, and 227.7 J g^{-1}, respectively. It can be calculated that the cumulative hydration heat in 3 days of the paste containing 30% FSS and FPS is reduced by 11.1 and 13.0%, respectively, which are both far below 30%. Thus, it can be concluded that FSS and FPS both have high activity.

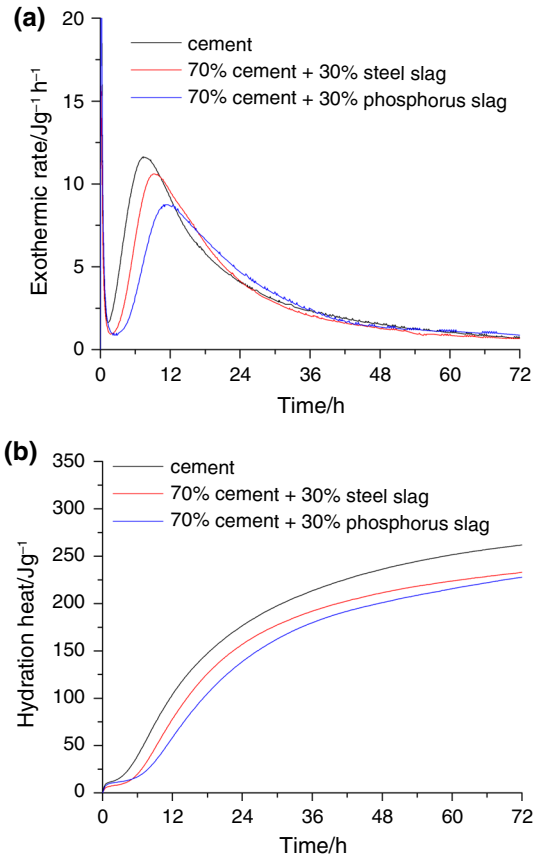

Fig. 3 Hydration heat of binder. **a** Exothermic rate; **b** cumulative heat

XRD results

Figures 4 and 5 show the XRD patterns of the hydrations products of the composite binder containing 30% fine steel slag and the composite binder containing 30% fine phosphorus slag hydrated for 360 and 720 days, respectively. C–S–H is the main hydration product. However, it is amorphous, and thus there is no characteristic peak for C–S–H in the XRD spectrum. $Ca(OH)_2$ and unhydrated

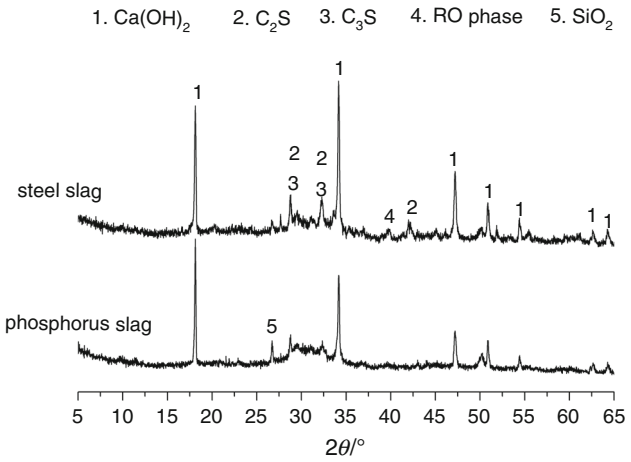

Fig. 4 XRD patterns of the hydration products of the composite binder containing fine steel slag and the composite binder containing fine phosphorus slag hydrated for 360 days

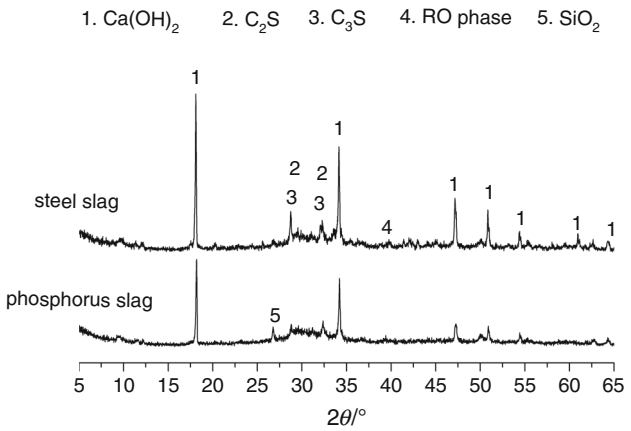

Fig. 5 XRD patterns of the hydration products of the composite binder containing fine steel slag and the composite binder containing fine phosphorus slag hydrated for 720 days

clinkers are the main crystalline phases in the plain cement paste as well as the composite pastes. The characteristic peak for RO phase can be seen in the XRD patterns of the hydration products of the composite binder containing fine steel slag. The characteristic peaks for SiO_2 can be seen in the XRD patterns of the hydration products of the composite binder containing fine phosphorus slag. It should be noted that the intensity of the peak of $Ca(OH)_2$ for the composite binder containing fine phosphorus slag is weaker than that for the composite binder containing fine steel slag, indicating that the $Ca(OH)_2$ content of the hydration products of the composite binder containing fine phosphorus slag is relative low.

Non-evaporable water content results

Non-evaporable water (w_n) content is the amount of water chemically bonded with the hydration products which is proportional to the amount of hydration products and is often used to determine the hydration degree of cement. The chemically bonded waters of different hydration products might vary significantly. It is not scientific to compare w_n contents of different binders directly due to their various hydration products, whereas for the same binder, w_n contents at different ages can be used to ascertain their degrees of hydration.

It can be seen from Table 3 that the increasing rates of w_n contents of all samples are relatively low after 90 days. In addition, the increasing rates of w_n contents from 90 to 360 days are all higher than those from 360 to 720 days. This is an indication that the rate of hydration decreases as the age grows. w_n contents of the pastes with the W/B ratio of 0.35 are all lower than those of the pastes with the W/B ratio of 0.45. This indicates that the lower the W/B ratio is, the smaller the space for hydration products to grow is, and the fewer hydration products are. However, the increasing rates of w_n contents of the pastes with the W/B ratio of 0.35 are all higher than those of the pastes with the W/B ratio of 0.45 after 90 days. This is believed to be due to that the hydration degree of the paste with a low W/B ratio at early stage is relatively low, so there are more unhydrated active components left for further hydration at late ages.

It can also be seen from Table 3 that after 90 days, the increasing rates of w_n contents of the pastes containing mineral admixtures are all higher than those of cement. What's more, the increasing rates of w_n contents increase with the contents of mineral admixtures increase. The reason may be that the activity of FSS and FPS is still lower than that of cement though it is higher than that of normal steel slag and phosphorus slag. As a result, FSS and FPS make great contributions to hydration of the composite binder at late age. The increasing rates of w_n contents of the pastes containing FPS are higher when compared with those of the pastes containing FSS which indicates that the increase amplitude of reaction degree of FPS is higher than that of FSS from 90 to 720 days.

TG/DTG results

There is a main mass loss from about 400–500 °C shown in TG–DTG curves of five kinds of composite binders at the age of 90, 360, and 720 days, respectively, which is due to the endothermic decomposition of $Ca(OH)_2$. The temperature of the endothermic decomposition of $Ca(OH)_2$ can be calculated accurately according to DTG curve, and then the mass percentage of $Ca(OH)_2$ can be calculated which is shown in Fig. 6.

As shown in Fig. 6, the content of $Ca(OH)_2$ in hydration products of cement increases with the age grows slowly after 90 days which is consistent with the result of w_n content. This is an indication that the hydration of cement has reached a high degree after 90 days. The main

Table 3 Non-evaporable water content and its increasing rate from 90 to 360 days and from 360 to 720 days

Samples	Non-evaporable water content/%			Increasing rate of non-evaporable water content/ %	
	90 days	360 days	720 days	From 90 to 360 days	From 360 to 720 days
C-0.45	16.94	17.36	17.61	2.48	1.44
S-0.45-15	16.61	17.13	17.47	3.13	1.98
S-0.45-30	16.03	16.72	17.13	4.30	2.45
P-0.45-15	16.36	16.97	17.46	3.72	2.89
P-0.45-30	15.88	16.69	17.21	5.10	3.11
C-0.35	14.88	15.39	15.75	3.43	2.34
S-0.35-15	14.66	15.35	15.84	4.71	3.19
S-0.35-30	14.15	14.99	15.55	5.94	3.74
P-0.35-15	14.47	15.15	15.79	4.70	4.22
P-0.35-30	14.04	14.99	15.77	6.77	5.20

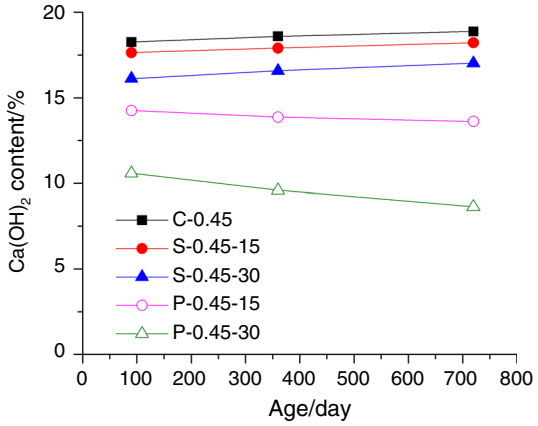

Fig. 6 $Ca(OH)_2$ content of the hydration products

hydration products of steel slag are C–S–H and $Ca(OH)_2$. The content of $Ca(OH)_2$ produced by steel slag is far less than that produced by cement with the same quantity. Furthermore, the reaction of steel slag does not consume $Ca(OH)_2$ during the hydration process of the composite binder containing steel slag. Consequently, the content of $Ca(OH)_2$ produced by the composite binder containing FSS increases slowly as the age grows. However, the content of $Ca(OH)_2$ in hydration products decreases with the replacement of FSS increases.

It can also be seen from Fig. 6 that the content of $Ca(OH)_2$ produced by the composite binder containing FPS is distinctly lower than that produced by cement after 90 days. The reason is that the content of cement in the composite binder decreases as the replacement of FPS increases and the content of $Ca(OH)_2$ produced is reduced correspondingly. In addition, the hydration products of FPS do not include $Ca(OH)_2$. On the contrary, FPS consumes $Ca(OH)_2$ during its hydration process. It is notable that the content of $Ca(OH)_2$ produced by the composite binder containing FPS decreases with the age grows which indicates that the consumption rate of $Ca(OH)_2$ by the reaction of FPS is higher than the production rate of $Ca(OH)_2$ by the hydration of cement. Meanwhile, it can also be observed that the content of $Ca(OH)_2$ produced by the composite binder containing FPS is obvious lower than that produced by the composite binder containing FSS with the same replacement ratio and the gap between them becomes larger with the replacement ratio increases.

MIP results

The cumulative pore volume curves of hardened pastes of five kinds of composite binders with the W/B ratio of 0.45 at the age of 720 days are depicted in Fig. 7a. It is evident that the cumulative pore volume and the proportion of pores between 30 and 200 nm increase with the replacement ratio of FSS increases. This indicates that the pore structure of hardened paste becomes coarser at late age by replacing part of cement with FSS. However, the proportion of pores smaller than 20 nm increases with the replacement ratio of FPS increases which indicates that FPS can improve the pore structure of hardened pastes at late age.

Figure 7b shows the cumulative pore volume curves of hardened pastes of five kinds of composite binders with the W/B ratio of 0.35 at the age of 720 days. The laws revealed by Fig. 7a, b are similar. The pore structure of the hardened paste containing FSS at 720 days becomes coarser as the replacement ratio of FSS increases. On the contrary, the pore structure of the hardened paste containing FPS at 720 days gets finer as the replacement ratio of FPS increases.

It can be concluded from Fig. 7 that the ability to improve the pore structure of the hardened paste containing FPS is better than that of the hardened paste containing FSS at late age. The results of TG–DTG have shown that

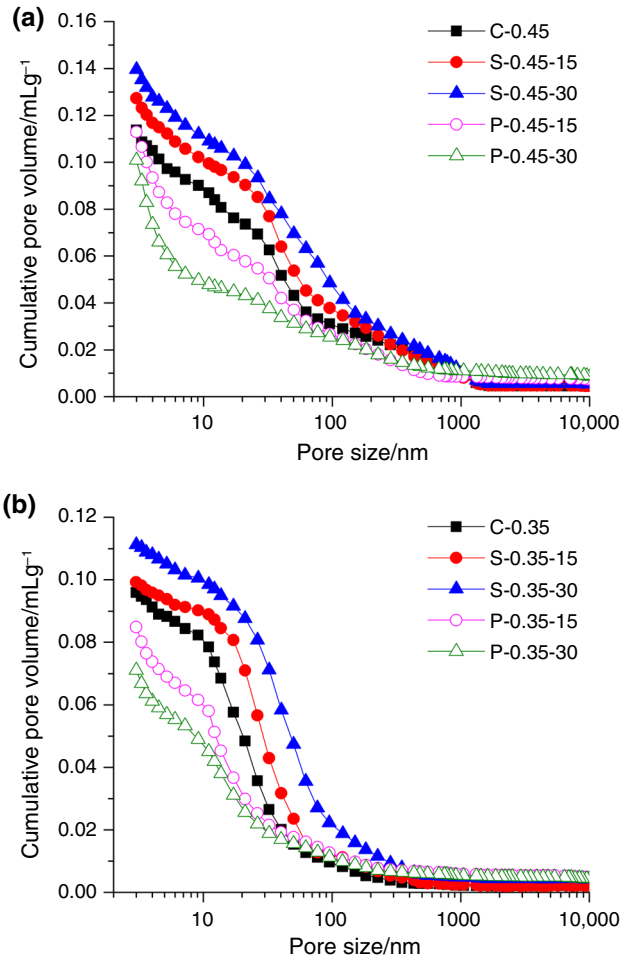

Fig. 7 Cumulative pore volume of hardened paste at 720 days. **a** W/B = 0.45; **b** W/B = 0.35

the ability to reduce the content of $Ca(OH)_2$ in hydration products of the composite binder containing FPS is much better than that of the composite binder containing FSS. $Ca(OH)_2$ in hydration products is known to occur as massive clusters or isolated hexagonal crystals [46]. The strength of $Ca(OH)_2$ is low, and its stability is very poor which gathers at the interfacial transition zone between cement and aggregates. As a result, the cohesive force at the interfacial transition zone between cement and aggregates is reduced and $Ca(OH)_2$ grain coarsening occurs which will become the weakest part in cementing materials [47, 48]. Therefore, the difference in hydration products between the composite binder containing FPS and FSS is one of the most important reasons for the difference in the influence they have on the pore structure. As for the hardened paste containing FSS, the amount of hydration products of FSS is smaller than that of the replaced cement. That is to say, the hydration products of the binder become less with the increase in FSS replacement ratio. What's more, the reaction of FSS does not consume $Ca(OH)_2$. Therefore, the addition of FSS tends to make coarser pore structure.

Strength

Figure 8a presents the compressive strengths of concrete of five kinds of composite binders with the W/B ratio of 0.45 at the age of 90, 360, and 720 days, respectively. At the age of 90 days, the compressive strength of concrete containing 15% FSS is slightly lower than that of pure cement concrete. However, the compressive strength of concrete containing 15% FPS is superior to that of pure cement concrete. In addition, the compressive strength of concrete containing 30% FSS or FPS is much lower than that of pure cement concrete and the concrete containing 30% FSS exhibits relatively lower compressive strength at 90 days. From the age of 90 days to 720 days, the compressive strength concrete with 15% FSS is similar to that of pure cement concrete. Meanwhile, the increase amplitude of compressive strength for concrete containing 15% FPS is higher than that for pure cement concrete during this period. The compressive strength of concrete with 30% FPS is similar to that of pure cement concrete at the age of 360 days and is close to that of concrete with 15% FPS at the age of 720 days. Although the gap of the compressive strength between concrete containing 30% FSS and pure cement concrete at the ages of both 360 and 720 days becomes smaller when compared to that at the age of 90 days, it is also very significant.

It can be seen from Fig. 8a that from the age of 90 days to 720 days, the increase amplitudes of compressive strengths for four kinds of composite binders containing FSS or FPS are all higher than that for pure cement concrete. The trend is consistent with that of w_n content (the increasing rates of w_n content of four kinds of composite binders containing FSS or FPS are all larger than those of pure cement during this period). The increase amplitude of compressive strength for concrete containing FPS is higher than that for concrete containing FSS with the same cement replacement ratio. The results are in accordance with those of w_n content (the increasing rates of composite binders containing FPS are all higher than those of composite binders containing FSS with the same replacement ratio during this period). Besides, the result of TG–DTG shows that the reaction of FPS consumes $Ca(OH)_2$ in hydration products while the reaction of FSS produces $Ca(OH)_2$ during this period. As a result, the improvement on the interfacial transition zone of concrete containing FPS is more significant than that of concrete containing FSS. At the age of 720 days, the compressive strength of concrete containing FPS is much higher than

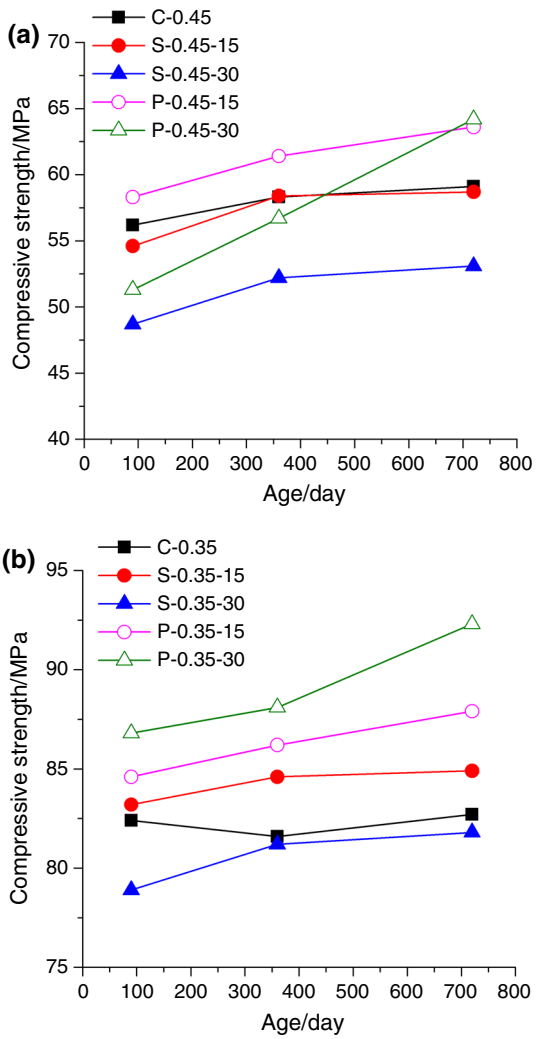

Fig. 8 Compressive strengths of concretes. **a** W/B = 0.45; **b** W/B = 0.35

that of concrete containing FSS with the same replacement ratio and the gap between them gets lager as the replacement ratio increases which consists with the result of the pore structure (Fig. 7a). Furthermore, the result of TG–DTG indicates that the content of $Ca(OH)_2$ in hydration products of the composite binder containing FSS is superior to that of the composite binder containing FPS with the same cement replacement ratio, and the gap between them becomes larger as the replacement ratio increases. It is also one of the most important reasons for the increase gap between their compressive strengths.

Figure 8b presents the compressive strengths of concrete of five kinds of composite binders with the W/B ratio of 0.35 at the age of 90, 360, and 720 days, respectively. Some laws revealed by Fig. 7a, b are similar. The increase amplitudes of compressive strengths for concrete containing FPS or FSS are all higher than those for pure cement concrete. The compressive strength of concrete containing FPS is distinctly higher than that of concrete containing FSS with the same replacement ratio regardless of age, and the gap between them gets larger with the replacement ratio and the age increase. It can also be seen from Fig. 8b that the compressive strength of concrete with 30% FPS is superior to that of pure cement concrete at the age of 90 days, and the compressive strength of concrete with 30% FSS is close to that of pure cement concrete at the ages of both 360 and 720 days, which are different from the result shown in Fig. 8a. This is because that the hardened paste gets denser and the porosity becomes lower as W/B ratio decreases which indicates that the negative effect that mineral admixtures have on the compressive strength of concrete weakens when used as a replacement of cement. On the other hand, the improvement on the interfacial transition zone of concrete has advantages to the compressive strength of concrete with a lower W/B ratio.

The splitting tensile strengths of concrete of five kinds of composite binders with the W/B ratio of 0.45 are presented in Fig. 9a. The splitting tensile strength of concrete with 15% FSS is slightly lower than that of pure cement concrete, and the splitting tensile strength of concrete with 30% FSS is obvious lower than that of pure cement concrete regardless of age. The splitting tensile strength of concrete with 15% FPS is superior to that of pure cement concrete at any age. In addition, the splitting tensile strength of concrete with 30% FPS is close to that of pure cement concrete at the ages of both 90 and 360 days but is distinctly higher than that of pure cement concrete at the age of 720 days. Note that the splitting tensile strength of concrete containing FPS is superior to that of concrete containing FSS with the same replacement ratio at any age and the difference between them increases with the replacement ratio and the age grow.

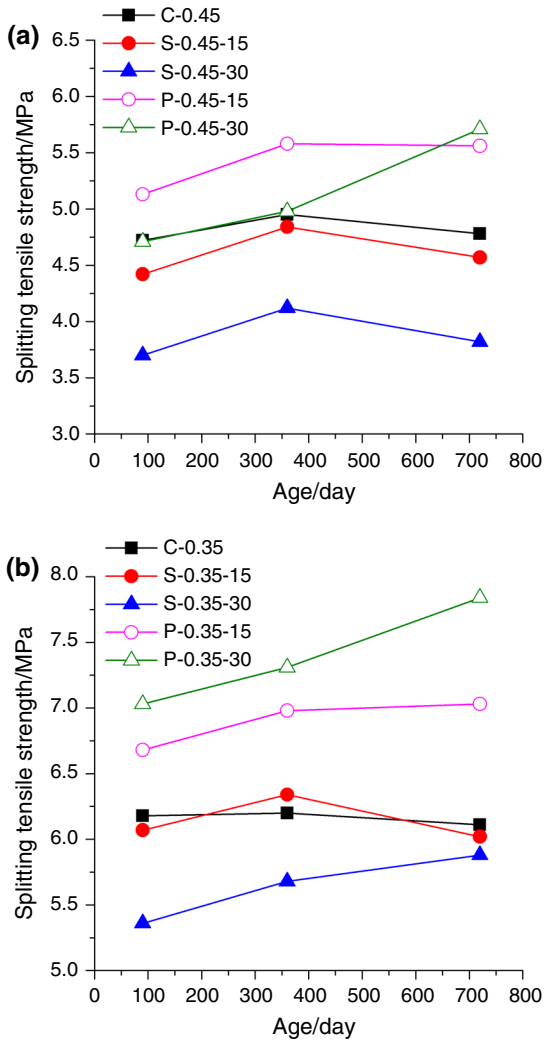

Fig. 9 Splitting tensile strengths of concretes. **a** W/B = 0.45; **b** W/B = 0.35

Figure 9b presents the splitting tensile strength of concrete of five kinds of composite binders with the W/B ratio of 0.35. Some laws revealed by Fig. 9a, b are similar. The splitting tensile strength of concrete containing FPS is superior to that of concrete containing FSS with the same replacement ratio, and the gap between them gets larger with the replacement ratio and the age increase. It can also be seen from Fig. 9b that the splitting tensile strength of concrete containing 30% FPS is obvious higher than that of pure cement concrete at the ages of both 90 and 360 days. It is noted that the splitting tensile strength of concrete containing 30% FPS is superior to that of concrete containing 15% FPS regardless of age. The splitting tensile strength of concrete containing 30% FSS is close to that of pure cement concrete at the age of 720 days which is different from the trend observed in Fig. 9a but is consistent with the result of the compressive strength (Fig. 8b).

Chloride ion permeability

Figure 10a shows the charge passed and permeability grade to chloride ion of concrete of five kinds of composite binders with the W/B ratio of 0.45. It is clear that the charge passed of them decreases as the age grows. At the age of 90 days, concrete containing 30% FSS exhibits high permeability while the other four kinds of concrete all exhibit moderate permeability. At the age of 360 days, the chloride ion permeability grade of concrete containing 30% FSS is moderate while concrete with 15% FSS, pure cement concrete, and concrete with 15% FPS still exhibit moderate permeability. Besides, the chloride ion permeability grade of concrete containing 30% FPS is low at 360 days. At the age of 720 days, concrete with 15% FSS, pure cement concrete, and concrete with 30% FSS still exhibit moderate permeability. In addition, concrete with 15% FPS exhibits low permeability and the chloride ion permeability grade of concrete with 30% FPS is still low.

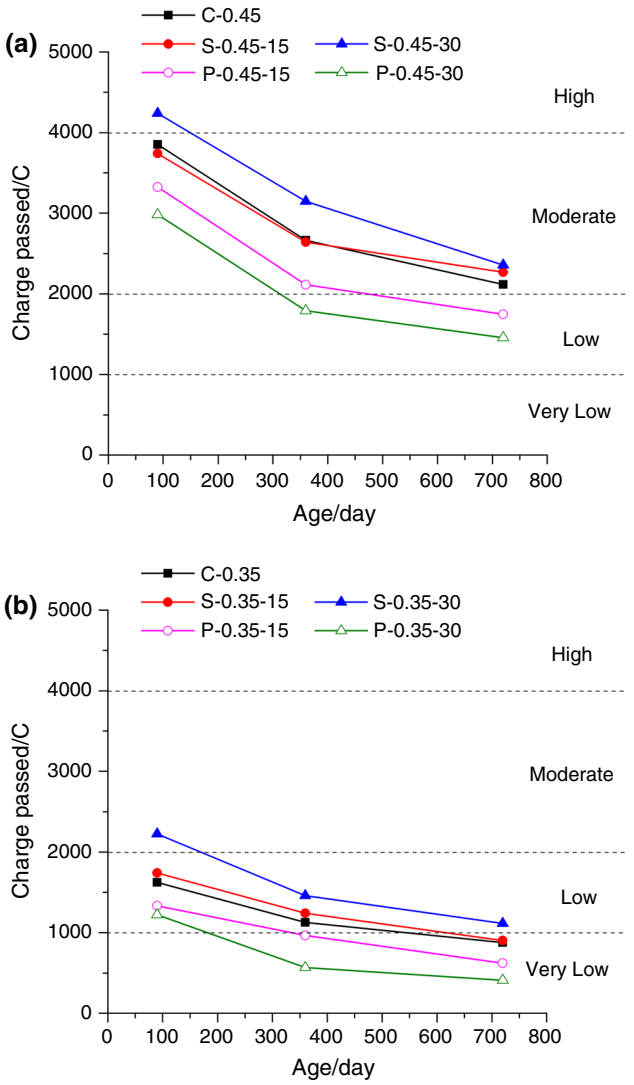

Fig. 10 Chloride ion permeability of concretes. **a** W/B = 0.45; **b** W/B = 0.35

Figure 10b shows the charge passed and permeability grade to chloride ion of concrete of five kinds of composite binders with the W/B ratio of 0.35. It is also clear that the charge passed of them decreases as the age grows. At the age of 90 days, the permeability grade to chloride ion of concrete with 30% FSS is one level higher than that of pure cement concrete which is consistent with the result under the condition of 0.45 W/B ratio and the same trend is observed at the age of 720 days. Concrete with 15% FSS exhibits the same permeability grade to chloride ion as pure cement concrete regardless of age. In addition, concrete containing FPS exhibits the same permeability grade as pure cement concrete at the age of 90 days but one level lower than pure cement concrete at the ages of both 360 and 720 days.

The conclusion can be drawn from Fig. 10a, b that FSS cannot improve the resistance to chloride ion penetration for concrete at late age while FPS can. The result of the pore structure shows that FPS can improve the pore structure of hardened pastes while FSS makes it coarse at late age which leads to the difference in the resistance to chloride ion penetration of concrete between them at late age. On the other hand, the interfacial transition zone of concrete has direct effects on the permeability to chloride ion. The reaction of FPS consumes $Ca(OH)_2$ and thus improves the interfacial transition zone of concrete which mainly contributes to the improvement of the resistance to chloride ion penetration on concrete at late age.

Carbonation depth

Figure 11 shows the carbonation depth of the concrete exposed in an accelerated carbonation chamber for 90 days after 28 days' initial standard curing. Under the condition of the W/B ratio of 0.45 and 0.35, both FSS and FPS replacement can result in an increase carbonation depth and the concrete containing FPS exhibits higher carbonation depth than that containing FSS with the same replacement ratio.

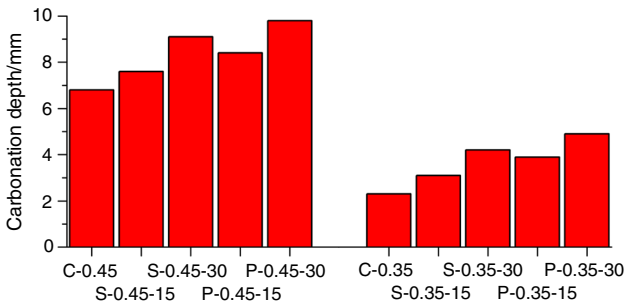

Fig. 11 Accelerated carbonation depth of concrete

Figure 12 presents the carbonation depth of the concrete exposed in nature for 720 days after 28 days' initial standard curing. With the W/B ratio of 0.45 and 0.35, both FSS and FPS replacement result in an increase carbonation depth which is in agreement with the result under the condition of the accelerated carbonation. However, the carbonation depth of the concrete containing FPS is smaller than that of the concrete containing FSS with the same replacement ratio which is contrary to the result under the condition of the accelerated carbonation.

It has been shown in the result of TG–DTG that both FPS and FSS replacement decrease $Ca(OH)_2$ content in hydration products which mainly accounts for their increase carbonation depth. In addition, the rate of carbonation is closely related to the degree of density of concrete. The lower the degree of density of concrete is, the lower the rate of carbonation is. Although $Ca(OH)_2$ content in hydration products of the composite binder containing FPS is lower than that of the composite binder containing FSS with the same replacement ratio, the pore structure of the hardened paste containing FPS is finer than that of the hardened paste containing FSS (Fig. 6), and the permeability grade to chloride ion of the concrete containing FPS is lower than that of the concrete containing FSS (Fig. 7). Therefore, the carbonation depth of the concrete containing FPS is lower than that of the concrete containing FSS exposed in nature. Neither reaction degree of FSS and FPS is high at the beginning of the accelerated carbonation experiment. Meanwhile, the improvement on the pore structure of FPS is not obvious at this time, so the result of the accelerated carbonation experiment mainly depends on $Ca(OH)_2$ content. As a result, the carbonation depth of the concrete containing FPS is higher than that of the concrete containing FSS exposed in the accelerated carbonation chamber. It can be concluded from the results of nature carbonation and accelerated carbonation that the difference in reaction kinetics between them is very large, of which the former is more credible.

It can be seen from Fig. 12 that the increase amplitude of carbonation depth of concrete containing 15% FSS or FPS is very small and thus little influence on the resistance to carbonation. However, FPS and FSS have a great influence on the resistance to carbonation when the replacement ratio is 30%.

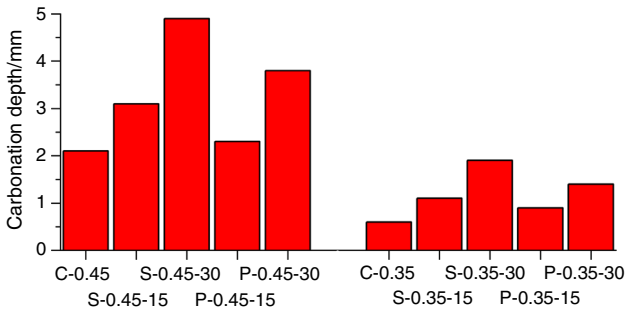

Fig. 12 Natural carbonation depth of concrete (carbonated for 720 days)

Sulfate attack

Figure 13a, b shows the strength loss rates of concretes with five different binders under sulfate attack for 90, 120, and 150 dry–wet circulation times with the W/B ratio of 0.45 and 0.35, respectively. A low-strength loss rate of concrete results from excellent resistance to sulfate attack. It is obvious that the strength loss rate at W/B ratio of 0.35 is much smaller than that at W/B ratio of 0.45 for the concretes with the same binder. It is an indication that the compactness which is closely related to the W/B ratio has a significant effect on the sulfate attack resistance of concrete. Figure 13a, b presents that the resistance to sulfate attack of concrete reduces with the replacement ratio of

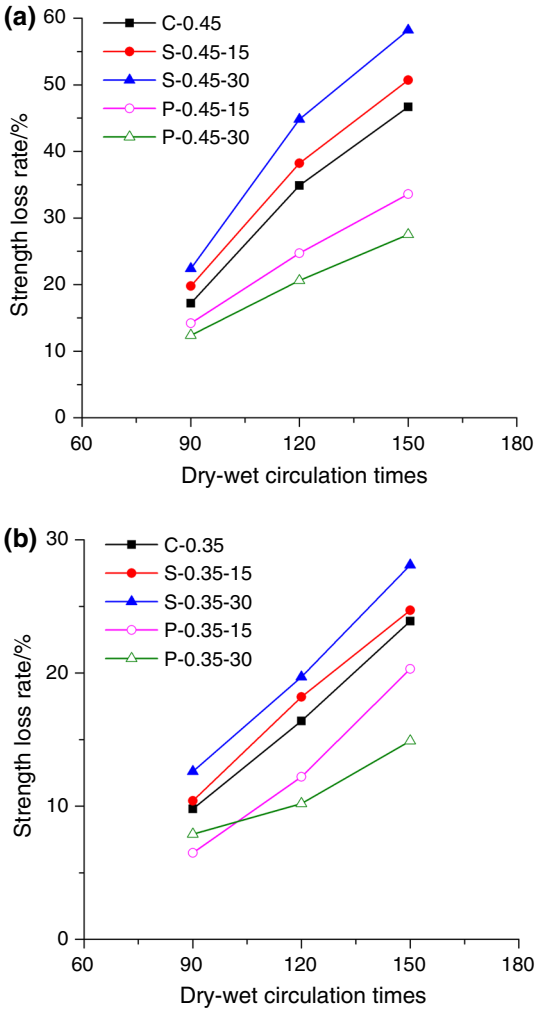

Fig. 13 Strength loss rate of concretes under sulfate attack. **a** W/B = 0.45; **b** W/B = 0.35

FSS increase and otherwise for the increase in replacement ratio of FPS.

The sulfate attack of concrete is mainly because the sulfate ion inside concrete reacts with $Ca(OH)_2$ and C–A–H which produces ettringite and gypsum, causing volume dilation and expansion cracking of concrete [49, 50]. The permeability of concrete counts on the rate of sulfate ion entering concrete. The result of the permeability of concrete experiment (Fig. 10) shows that FPS can improve the permeability of concrete significantly while FSS has negative effects on it. In addition, as shown in the result of TG–DTG (Fig. 6), FPS can reduce $Ca(OH)_2$ content in hydration products obviously while FSS cannot. The crystallization of sulfates, which induces expansion stress, is another factor causing damage of concrete structure. Denser structure tends to slow down the penetration of sulfate ions and thus release the chemical effect as well as crystallization effect of sulfates. What's more, the cracking of concrete would accelerate the penetration of sulfate ions significantly, which would increase the crystallization effect of sulfates significantly. So, reducing or delaying the cracking of concrete is beneficial to the prevention of the crystallization of sulfates. As a result, FPS is much helpful to the resistance to sulfate attack of concrete while FSS has an adverse effect on the resistance to sulfate attack of concrete and the law revealed above is more obvious as the replacement ratio increases.

Conclusions

1. Replacing 30% of the cement by FSS and FPS can both prolong the dormant period of hydration evolution, and the retarding effect of FPS is more significant relatively. The increase amplitude of reaction degree of FPS is higher than that of FSS, and both of them are higher than that of pure cement from 90 to 720 days.
2. The ability to improve the pore structure of FPS is better than that of FSS, and the content of $Ca(OH)_2$ in hydration products of FPS is lower than that of FSS at the age of 720 days. As a result, FPS can improve the resistance to chloride ion penetration for concrete at late age (after 90 days) while FSS cannot.
3. FPS has advantages to the development of compressive strength and splitting tensile strength of concrete as the age and the replacement ratio grow at late ages when compared to pure cement and FSS, which is more significant under the condition of lower W/B ratio (W/B ratio of 0.35).
4. Based on the result of nature carbonation which is more credible, both FSS and FPS replacement result in an obvious increase carbonation depth with 30% replacement ratio when compared to that of pure cement concrete, and the carbonation depth of the concrete containing FPS is smaller than that of the concrete containing FSS with the same replacement ratio at 720 days.
5. FPS is much more beneficial to the resistance to sulfate attack of concrete while FSS is more disadvantageous to the resistance to sulfate attack of concrete as the replacement ratio increases in the long term (after 90 days).

Acknowledgements Authors would like to acknowledge the Key Project of Natural Science Foundation of SiChuan Education Department of China (16ZA0431).

References

1. Ahari RS, Erdem TK, Ramyar K. Time-dependent rheological characteristics of self-consolidating concrete containing various mineral admixtures. Constr Build Mater. 2015;88:134–42.
2. Sotiriadis K, Nikolopoulou E, Tsivilis S, Pavlou A, Chaniotakis E, Swamy RN. The effect of chlorides on the thaumasite form of sulfate attack of limestone cement concrete containing mineral admixtures at low temperature. Constr Build Mater. 2013;43:156–64.
3. Irassar EF, Maio AD, Batic OR. Sulfate attack on concrete with mineral admixtures. Cem Concr Res. 1996;26(1):113–23.
4. Skaropoulou A, Tsivilis S, Kakali G, Sharp JH, Swamy RN. Thaumasite form of sulfate attack in limestone cement mortars: a study on long term efficiency of mineral admixtures. Constr Build Mater. 2009;23(6):2338–45.
5. Uysal M, Yilmaz K. Effect of mineral admixtures on properties of self-compacting concrete. Cement Concr Compos. 2011;33(7):771–6.
6. Ye G, Liu X, Schutter GD, Poppe AM, Taerwe L. Influence of limestone powder used as filler in SCC on hydration and microstructure of cement pastes. Cement Concr Compos. 2007;29(2):94–102.
7. Poppe AM, Schutter GD. Cement hydration in the presence of high filler contents. Cem Concr Res. 2005;35(12):2290–9.
8. Assié S, Escadeillas G, Waller V. Estimates of self-compacting concrete 'potential' durability. Constr Build Mater. 2007;21(10):1909–17.
9. Duan P, Shui Z, Chen W, Shen C. Efficiency of mineral admixtures in concrete: microstructure, compressive strength and stability of hydrate phases. Appl Clay Sci. 2013;83–84:115–21.
10. Alibert JJ, Seppecher P. Study of the durability of OPC versus GGBS concrete on exposure to silage effluent. J Mater Civ Eng. 2008;20(4):313–20.
11. Vargas JA. A designer's view of fly ash concrete. Concr Int. 2007;29(2):43–6.
12. Shao Y, El-Baghdadi A, He Z, Mucci A, Fournier B. Carbon dioxide-activated steel slag for slag-bonded wallboard application. J Mater Civ Eng. 2015; 27(3). doi:10.1061/(ASCE)MT.1943-5533.0001055.
13. Zhang TS, Yu QJ, Wei JX, Li JX. Investigation on mechanical properties, durability and micro-structural development of steel slag blended cements. J Therm Anal Calorim. 2012;110:633–9.
14. Zhang TS, Yu QJ, Wei JX, Zhang PP. Efficient utilization of cementitious materials to produce sustainable blended cement. Cement Concr Compos. 2012;34(5):692–9.
15. Wang Q, Shi MX, Yang J. Influence of classified steel slag with particle sizes smaller than 20 μm on the properties of cement and concrete. Constr Build Mater. 2016;123:601–10.

16. Hu SG, He YJ, Lu LN, Ding QJ. Effect of fine steel slag powder on the early hydration process of portland cement. J Wuhan Univ Technol Mater Sci. 2006;21(1):147–9.
17. Wang Q, Yan PY, Mi G. Effect of blended steel slag—GBFS mineral admixture on hydration and strength of cement. Constr Build Mater. 2012;35(10):8–14.
18. Wang Q, Yan PY, Feng J. A discussion on improving hydration activity of steel slag by altering its mineral compositions. J Hazard Mater. 2011;186(2–3):1070–5.
19. Li YF, Liu SA, Du RQ, Kong FY. Effectiveness of steel slag powder on suppressing alkali aggregate reaction of concrete. Adv Mater Res. 2009;79–82:179–82.
20. Wang Z, Liu S, Li X. Long-term properties of concrete containing ground granulated blast furnace slag and steel slag. Mag Concr Res. 2014;66(21):1–9.
21. Tsakiridis PE, Papadimitriou GD, Tsivilis S, Tsivilis S, Koroneos C. Utilization of steel slag for Portland cement clinker production. J Hazard Mater. 2008;152(2):805–11.
22. Guo XL, Shi HS, Wu K. Effects of steel slag powder on workability and durability of concrete. J Wuhan Univ Technol. 2014;29(4):733–9.
23. Wang K, Qian C, Wang R. The properties and mechanism of microbial mineralized steel slag bricks. Constr Build Mater. 2016;113:815–23.
24. Singh NB, Bhattacharjee KN. Phosphorus furnace slag—a potential waste material for the manufacture of cements. Indian J Eng Mater Sci. 1996;3:41–4.
25. Liu XW, Yang L, Zhang B. Utilization of phosphorus slag and fly ash for the preparation of ready-mixed mortar. Appl Mech Mater. 2013;423–426:987–92.
26. Peng Y, Zhang J, Liu J, Ke J, Wang F. Properties and microstructure of reactive powder concrete having a high content of phosphorous slag powder and silica fume. Constr Build Mater. 2015;101:482–7.
27. Li D, Shen J, Mao L, Wu X. The influence of admixtures on the properties of phosphorous slag cement. Cem Concr Res. 2000;30(7):1169–73.
28. Allahverdi A, Abadi MMBR, Hossain KMA, Lachemi M. Resistance of chemically-activated high phosphorous slag content cement against freeze–thaw cycles. Cold Reg Sci Technol. 2014;98(2):107–14.
29. Li DX, Chen L, Xu ZZ, Luo ZM. A blended cement containing blast furnace slag and phosphorous slag. J Wuhan Univ Sci Technol Mater Sci Ed. 2002;17(2):62–5.
30. Her JW, Lim NG. Physical and chemical properties of nano slag mixed mortar. J Korea Inst Build Constr. 2010;10(6):145–54.
31. Lim NG. The study on properties of concrete using high-Blaine blast-furnace slag powder. J Korea Inst Archit. 2005;49(10):119–29.
32. Zhu X, Hou H, Huang X, Zhou M, Wang W. Enhance hydration properties of steel slag using grinding aids by mechanochemical effect. Constr Build Mater. 2012;29(4):476–81.
33. Shi MX, Wang Q, Zhou ZK. Comparison of the properties between high-volume fly ash concrete and high-volume steel slag concrete under temperature matching curing condition. Constr Build Mater. 2015;98:649–55.
34. Wang Q, Yang JW, Yan PY. Cementitious properties of superfine steel slag. Powder Technol. 2013;245(8):35–9.
35. Hu SG, He YJ, Lu LN, Ding QJ. Effect of fine steel slag powder on the early hydration process of Portland cement. J Wuhan Univ Technol Mater Sci Ed. 2006;21(1):147–9.
36. Liu S, Li L. Influence of fineness on the cementitious properties of steel slag. J Therm Anal Calorim. 2014;117(2):629–34.
37. Shi Y, Chen HY, Wang J. Effects of ultrafine grinded steel slag addition on properties of cement. Mater Sci Forum. 2014;804:67–70.
38. Feng JJ, Wang XQ, Wang SS. The influence of super-fine steel slag on the properties of high-strength concrete. Appl Mech Mater. 2013;477–478:941–4.
39. Cheng L, Zhu C, Sheng G. Mechanical properties and microstructures of alkali-activated phosphorous slag cement. J Chin Ceram Soc. 2006;34(5):604–9.
40. Gao P, Lu X, Yang C, Li XY, Shi NN, Jin SC. Microstructure and pore structure of concrete mixed with superfine phosphorous slag and superplasticizer. Constr Build Mater. 2008;22(5):837–40.
41. ASTM C1202-12, Standard test method for electrical indication of concrete's ability to resist chloride ion penetration. American Society for Testing and Materials, Annual Book of ASTM Standards, 2012.
42. GB/T 50082-2009, Standard for test methods of long-term performance and durability of ordinary concrete. Beijing: China Building Industry Press, 2009.
43. Wang Q, Yan PY, Han S. The influence of steel slag on the hydration of cement during the hydration process of complex binder. Sci China Technolog Sci. 2011;54(2):388–94.
44. Allahverdi A, Mahinroosta M. Mechanical activation of chemically activated high phosphorous slag content cement. Powder Technol. 2014;245(8):182–8.
45. Chen JS, Zhao B, Wang XM, Zhang QL, Wang L. Cemented backfilling performance of yellow phosphorous slag. Int J Miner Metall Mater. 2010;17(1):121–6.
46. Han S, Yan PY, Liu RG. Study on the hydration product of cement in early age using TEM. Sci China Technolog Sci. 2012;55(8):2284–90.
47. Gallucci E, Scrivener K. Crystallisation of calcium hydroxide in early age model and ordinary cementitious systems. Cem Concr Res. 2007;37(4):492–501.
48. Harutyunyan VS, Kirchheim AP, Monteiro PJM, Aivazyan AP, Fischer P. Investigation of early growth of calcium hydroxide crystals in cement solution by soft X-ray transmission microscopy. J Mater Sci. 2009;44(4):962–9.
49. Tian B, Cohen MD. Does gypsum formation during sulfate attack on concrete lead to expansion? Cem Concr Res. 2000;30(1):117–23.
50. Santhanam M, Cohen MD, Olek J. Effects of gypsum formation on the performance of cement mortars during external sulfate attack. Cem Concr Res. 2003;33(3):325–32.